HHS Public Access

Author manuscript

Biochim Biophys Acta. Author manuscript; available in PMC 2018 September 01.

Published in final edited form as:

Biochim Biophys Acta. 2017 September ; 1863(9): 2355–2362. doi:10.1016/j.bbadis.2017.06.022.

High glucose-induced p53 phosphorylation contributes to impairment of endothelial antioxidant system

Yong Wu[1,2], **Sangkyu Lee**[1], **Selene Bobadilla**[1], **Sheng Zhong Duan**[3,4], and **Xuan Liu**[1]

[1]Department of Biochemistry, University of California, Riverside, California 92521

[3]Key Laboratory of Nutrition and Metabolism, Institute for Nutritional Sciences, Shanghai

[4]Institutes for Biological Sciences, Chinese Academy of Sciences, Shanghai, China

Abstract

High levels of glucose (HG) induce reactive oxygen species-mediated oxidative stress in endothelial cells (ECs), which leads to endothelial dysfunction and tissue damage. However, the molecular mechanisms involved in HG-induced endothelial oxidative stress and damage remain elusive. Here we show that cellular ATP level-modulated p53 Thr55 phosphorylation plays a critical role in the process. Upon HG exposure, the elevated ATP levels induced the kinase activity of TAF1 (TBP-associated factor 1), which leads to p53 Thr55 phosphorylation. The phosphorylation dissociates p53 from the glutathione peroxidase 1 (GPX1) promoter and results in reduction of GPX1 expression. Inhibition of TAF1-mediated p53 Thr55 phosphorylation abolished those events, supporting the role of TAF1 in sensing cellular ATP elevation and in regulating GPX1 expression under the HG condition. Importantly, treating cells with HG increased intracellular H_2O_2 and cell apoptosis, as well as suppressed nitric oxide (NO) bioavailability and tube network formation. These effects were also remarkably reversed by inhibition of TAF1 and p53 Thr55 phosphorylation. We conclude that HG leads to endothelial dysfunction via TAF1-mediated p53 Thr55 phosphorylation and subsequent GPX1 inactivation. Our study thus revealed a novel mechanism by which HG induces endothelial oxidative stress and damage and possibly provided an avenue for targeted therapy for diabetes-associated cardiovascular diseases.

Keywords

p53; Thr55 phosphorylation; TAF1; high glucose; cellular ATP; GPX1

Introduction

Diabetes mellitus can cause multiple vascular complications and cardiovascular dysfunction. [1] A number of important epidemiological studies have highlighted the relationship between

Corresponding author: xuan.liu@ucr.edu; TEL: (951) 827-4350; FAX: (951) 827-4434.

[2]Current address: Charles R. Drew University of Medicine and Science, Los Angeles, CA 90059; David Geffen School of Medicine, University of California, Los Angeles, CA 90095

hyperglycemia (high blood glucose, HG) and an increased risk of cardiovascular diseases.[2, 3] HG induces reactive oxygen species (ROS)-mediated oxidative stress in endothelial cells (ECs), which leads to endothelial dysfunction and tissue damage.[4, 5] These events, in theory, could contribute to the pathogenesis of vascular diseases in diabetics. In addition, intensive glucose control effectively reduces the risk of microvascular complications of diabetes such as retinopathy, neuropathy, and nephropathy.[3] Despite its significance, the precise molecular mechanisms by which hyperglycemia induces endothelial oxidative stress and damage remained largely undefined. With the onset of diabetes and the development of its complications becoming earlier, knowledge of the body's response to glucose challenge is urgently needed.

The p53 tumor suppressor plays a critical role in the cellular response to stress.[6, 7] Apart from its important role in tumor suppression, p53 is also implicated in diabetes-associated complications,[8, 9] endothelial dysfunction[10] and arthrosclerosis.[11] Recent studies have shown that p53 might play a critical role in regulating ROS production in cultured cells.[12] Under normal growth conditions, p53 is required for maintaining basal transcription of antioxidant genes SESN1, SESN2, and GPX1.[12, 13] Suppression of p53 significantly decreases the basal transcriptions of those genes,[13] which increases cellular ROS levels and subsequently leads to oxidative damage of DNA. Thus regulating antioxidant defense to reduce ROS levels may represent one of the important tumor suppressing and cardiovascular protecting mechanisms of p53.

Previous studies from our laboratory indicated that p53 is phosphorylated at Thr55 by TAF1 and this phosphorylation leads to p53 inactivation.[14, 15] TAF1 is the largest subunit of transcription factor TFIID, which is composed of the TATA binding protein (TBP) and 13 to 14 TBP-associated factors (TAFs).[16, 17] Unlike other p53 kinases, TAF1 can phosphorylate p53 on the promoter, leading to p53 protein degradation [14] and inactivation.[18] Intriguingly, presumably due to TAF1's high K_m value for ATP, TAF1-mediated p53 phosphorylation is modulated by cellular ATP levels. Since hyperglycemia might increase cellular ATP levels in ECs, potentially leading to p53 Thr55 phosphorylation and subsequently inhibition, we hypothesize that it might contribute to HG-induced cardiovascular dysfunction. To test this possibility, we treated HAEC with HG and indeed observed an HG-induced ATP increase in ECs. Significantly, increased ATP level enhanced TAF1 kinase activity and p53 Thr55 phosphorylation in ECs. Upon Thr55 phosphorylation, p53 dissociated from the GPX1 promoter, which leads to reduction of antioxidant gene GPX1 expression and resultant oxidative stress in ECs. These results suggest that hyperglycemia can increases oxidative stress via TAF1-mediated and p53-dependent impairment of antioxidant defense mechanism.

Material and methods

Cell Culture

Human umbilical vein endothelial cells (HUVEC) and human aortic endothelial cells (HAEC) (both at passage 3) were purchased from Lonza (Walkersville, MD, USA) and were growth in Lonza's EGM-2 and EGM-MV at 37 °C in an atmosphere of 95% air–5% CO2. HUVEC and HAEC from passages 2–5 were cultured for 0–48 hours and treated with various concentrations of glucose (Boston BioProducts), 15 mM mannitol (Sigma), 25 mM

2-deoxyglucose (2-DG, Calbiochem), 30 μM apigenin (Sigma), 500 U/mL PEG-catalase (Sigma) or 20 μM proteasome inhibitor MG132 (A.G Scientific). HUVEC used in the experiments was the same batch at different passage (passage 4–7). Results of multiple observations using HAEC are presented as representative results from three different batches of cells.

Western blot and immunoprecipitation analysis

Whole-cell extract was prepared by lysing the cells in lysis buffer containing 20 mM Tris-Cl (pH 7.9), 150 mM NaCl, 0.5% NP-40, 20% glycerol, 2 mM EDTA, 0.5 mM DTT, 2 μg/ml aprotinin, 2 μg/ml leupeptin, and 0.5 mM PMSF. Cell lysates were subjected to SDS-PAGE followed by IB with antibodies as indicated. To detect p53 phosphorylation at Thr55, the cell lysate was immunoprecipitated with phosphor-specific antibody for Thr55 (Ab202) and immunoblotted with anti-p53 (DO-1) antibody. To normalize the p53 protein levels, 20 μM MG132 was applied. Other antibodies used in the present study and their commercial sources were as follows: anti-p53 antibody (DO1) was purchased from Santa Cruz Biotechnology; anti-GPX1, anti-phospho-Ser15, anti-phospho-Ser20 and anti-Cleaved caspase-3 antibodies were from Cell Signaling Technology; anti-phospho-Thr55 antibody ($Ab202^{15}$) and anti-TAF1 antibody (Ab1230) were homemade; anti-vinculin antibody (VIN-11-5) was from Sigma.

Measurement of reactive oxygen species

To detect intracellular reactive oxygen species (ROS), the ROS-sensitive fluorescent indicator 2′,7′-dihydrodichlorofluorescin diacetate (DCFDA, Molecular Probes) was used as described previously.[19] Confluent HAEC in 96-well plates were preincubated with 10 μM DCFDA for 30 min. After removal of medium from wells, cells were washed in PBS, followed by measurement of fluorescence intensity at 485-nm excitation and 538-nm emission spectra with a fluorescence microplate reader. Data are presented as a fold increase in DCF fluorescence compared with that in unstimulated cells.

Chromatin immunoprecipitation (ChIP) analysis

ChIP analysis to determine the binding of p53 on the GPX1 promoter was carried out as described previously.[20] In brief, HAECs were fixed with 1% formaldehyde. Chromatin immunoprecipitation was carried out with an anti-p53 (FL393, Santa Cruz) antibody and analyzed by PCR using a pair of primers (Forward: 5′-CCTAACTCAGGAACCTCTGAGAAA; reverse: 5′-CAGGAAAAGGCTGGAGAGTG) covering a putative p53 binding site on the promoter. The PCR products were electrophoresed by agarose gels and visualized by ethidium bromide.

ATP detection

Intracellular ATP level was measured by a luciferin/luciferase method using an ATP determination kit according to manufacturer's protocol (Molecular Probes). A standard curve was generated from known concentrations of ATP in each experiment and used to calculate ATP in each sample. The data were normalized by protein concentrations. The

results were expressed as fold (means ± S.D.) over untreated cells (mock) from three independent experiments.

TAF1 siRNA gene silencing

TAF1 siRNA (5′-AAGACCCAAACAACCCCGCAT-3′) or control siRNA was transfected into EC using BioT transfection reagent (Bioland Scientific LLC, Cerritos, CA). For rescue experiments, cells were also transfected with siRNA-resistant TAF1 (pCMV-HARecTAF1) that contains four silent mutations within TAF1–specific siRNA target sequence as underlined (5′-AAGACCCAAACAACCCCGCAT-3′). Cell transfection was performed using TransPass HUVEC Transfection Reagent (New England Biolabs) with 2 μg Rec TAF1, 4 μg TAF1 kinase dead mutant A2/N7 Ala (KD/A2), and 1 μg of p53 WT, p53 T55A, or empty vector.

Cloning and Expression of GPX1

The GPX1 cDNA was generated from total RNA extracted from HUVEC using the SuperScript™ One-Step RT-PCR with Platinum Taq kit (Invitrogen). Gene specific primers were designed based on the human GPX1 sequence (GenBank accession number NM_000581.2) and incorporated BamHI and XbaI for cloning (5′-ACTGTAGGATCC CAGTTAAAAGGAGGCGCCTGCTGGCCT and 5′-TGACATTCTAGAAGTGGGGAAACTCGCCTTGGTCTGGCA). The cDNA including a portion of the 5′UTR and most of the 3′UTR including selenocysteine-insertion sequence (SECIS) motif [21] was cloned into pcDNA 3.1 (Invitrogen) to generate pcDNA3.1/gpx1. To express GPX1, ECs were transfected with 1 μg pcDNA3.1/gpx1 using TransPass HUVEC™ Transfection Reagent.

TAF1 kinase assay

HAECs were washed with ice-cold PBS containing 1 mM Na_3VO_4 and 1 mM NaF and scraped on ice in 400 μl of 1:5 diluted buffer A (50 mM Hepes, pH 7.4, 1 mM EDTA, 10 mM mannitol, 1 mM DTT, 1 mM Na_3VO_4, 1 mM NaF, 5 μM microcystin, 5 nM okadaic acid, 2μg/ml aprotinin, 2μg/ml leupeptin, and 1 mM PMSF) and homogenized with 25 G needle for 10 strokes. After brief centrifugation at 6,000 × *g* at 4°C, The pellet was collected and washed with buffer A and then suspended in 500 μL of lysis buffer plus 1 mM Na_3VO_4, 1 mM NaF, 10 mM Na_2MoO_4, 20 mM β-glycerophosphate, 5 μM microcystin, 5 nM okadaic acid. After centrifugation, the supernatant (nuclear fraction) was collected and used for TAF1 immunoprecipitation. Cell lysates containing 1 mg protein were incubated with TAF1 antibodies (Ab1230) at 4°C for 3 h. After immunoprecipitation, the samples were washed once with ice-cold lysis buffer, once with lysis buffer containing 500 mM NaCl, once with phosphorylation buffer (20 mM HEPES, 12.5 mM $MgCl_2$, 100 mM KCl, and 1 mg/ml BSA, pH 7.9) and suspended in 40 μl of phosphorylation buffer. Kinase reactions were carried out at 30°C for 30 min using 120 ng of purified p53 as substrates in phosphorylation buffer. Thr55 phosphorylation of p53 was detected using anti-Thr55-Phos (Ab202).

RT-PCR and qRT-PCR

Total RNA was extracted using TRIzol reagent (Sigma), and RT-PCR was performed using SuperScript One-Step RT-PCR kit (Invitrogen) according to manufacturer's protocol. Primers used to amplify GPX1 mRNA are 5′-GTTTGGGCATCAGGAGAACGCCA-3′ and 5′-CGCACCGTTCACCTCGCACTT-3′. qRT-PCR was performed using iQ™ SYBRR® Green supermix and the iScript cDNA synthesis kit (Bio-Rad, USA) on Bio-Rad CFX96 Real Time System (Bio-Rad Laboratories) according to manufacturer's protocol.

Cell Apoptosis Analysis

Following various treatment, HAECs were collected, treated with 500 μg/ml of RNase A (Sigma), stained with 50 μg/ml of propidium iodide (Sigma) for 30 min at room temperature and subsequently analyzed by FACScan flow cytometry (Becton Dickinson) for apoptotic cells (subG1) according to DNA content.

Nitric Oxide Release

NO quantification was performed using the NO-specific fluorescent dye 4,5-diaminofluorescein diacetate (DAF-2 DA; Cayman Chemical, Ann Arbor, MI) as described previously.[22] Briefly, HAEC were seeded in 96-well plates (3×10^4 cells/well), cultured for 24 h and then serum starved for 2 h in phenol red-free EBM supplemented with L-arginine (100 μM) and uric acid (UA, 100 μM). Cells were then loaded with DAF-2 DA (5 μM final concentration) for 10 min at 37°C. After being loaded with DAF-2 DA, cells were washed three times with EBM at 37°C and kept in the dark. The fluorescence intensity was measured with a multilabel plate reader Wallac 1420 VICTOR2 (PerkinElmer) using 485 nm as excitation and 535 nm as emission wavelengths. The fluorescence intensities were corrected by subtracting the non-specific fluorescence in wells either without addition of DAF-2 DA or without cells.

Endothelial tube formation

Tube formation was assayed as previously described.[23] In brief, HAECs were seeded at 75,000 cells/well in 24-well cluster plates coated with 200 μl of Matrigel basement membrane matrix (BD Biosciences, Bedford, MA) for 24 hours. Photomicrographs were acquired on a stereo microscope (Leica MZIII) and number of capillary-like networks[24] for three fields of view (×100 magnification) were counted per well.

Statistical Analysis

All results were analyzed with unpaired Student *t* test or 1-way ANOVA, except for those obtained from the time-course studies, which were analyzed with repeated-measures ANOVA. Values are expressed as mean±SD for all assays. Significance was accepted at $P<0.05$.

Results

High glucose treatment inhibits GPX1 expression through p53 and leads to ROS accumulation in HAECs

Since blood glucose levels can range from 5.6 to 20 mM in hyperglycemia (American Diabetes Association guidelines), we first exposed HAECs to 20 mM high glucose (HG) for 48 hours and assayed cellular ROS level as well as GPX1 protein levels (Fig. 1*A*). Compared to 5 mM glucose control (M), exposure of cells to HG led to a significant increase in cellular ROS level (as measured by H_2O_2 levels) after the treatment as well as a parallel reduction in GPX1 protein level ($p<0.01$). To better establish a dose-dependent effect, we treated HAECs with 5 to 25 mM glucose (Fig. S1*A*). Decreased GPX1 protein levels as well as increased cellular ROS levels were clearly detected with 15 mM glucose and the maximum level of effect was observed at 25 mM glucose. As an osmotic control, exposure of HAECs to 5 mM glucose plus 15 mM mannitol had no effect on GPX1 protein level (Fig. 1*B*).

To define molecular mechanism by which HG induces endothelial oxidative stress and damage, we also assayed p53 protein level upon HG exposure since it is a transcription activator for GPX1. The assay clearly showed a corresponding down-regulation of p53 protein level upon HG exposure (Fig. 1*A*, S1*A*). To ensure the HG-induced GPX1 reduction was indeed mediated through p53, we knock-downed p53 by specific small interfering RNA (p53-siRNA) and showed that GPX1 protein levels decreased significantly even without HG treatment, implying that p53 play an important role in maintaining of GPX1 protein levels (Fig. 1*C*). Importantly, under this condition, HG-induced GPX1 reduction was abolished (Fig. 1*C*). To further confirm the role of p53, we showed overexpression of p53 rescued HG-induced GPX1 reduction (Fig. 1*D*). To verify the role of p53 as a transcription activator to regulate GPX1 in response to HG, we performed RT-PCR and qRT-PCR analyses and showed that the GPX1 is regulated at transcription level in HAECs (Fig. 1*E*). Together, our data indicate that treating cells with high glucose inhibits p53, which leads to suppression of GPX1 expression and accumulation of ROS in HAECs.

HG treatment elevates ATP level and enhances p53 Thr55 phosphorylation in HAECs

We previously reported that, upon DNA damage, p53 transcriptional activity is affected by cellular ATP level through Thr55 phosphorylation in human osteosarcoma U2OS cells.[18] We thus assayed whether HG inhibits p53 via altering cellular ATP levels and Thr55 phosphorylation in HAECs. Treating HAECs with HG indeed increases cellular ATP level in a time- and dose-dependent manner, and importantly, concurrent with increased cellular ATP levels, increased p53 Thr55, but not other, phosphorylation was indeed evident upon HG exposure (Fig. 2*A* and S2*A*). Treating cells with 2-deoxyglucose (2-DG), an inhibitor of glucose metabolism,[25] eliminated HG-induced ATP elevation and p53 Thr55 phosphorylation (Fig. 2*B*), suggesting glucose metabolism is required for the effect. Importantly, 2-DG treatment also effectively blocked HG-induced GPX1 reduction at both protein (Fig. 2*B*) and mRNA levels (Fig. S2*C*) as well as ROS accumulation (Fig. 2*C*). Treating cells with 2-DG alone has no effect on p53 and GPX1 (Fig. S2*B*). These results

suggest that HG exposure increases cellular ATP level and p53 Thr55 phosphorylation, which leads to p53 inactivation, GPX1 suppression and ROS accumulation in HAECs.

TAF1 kinase activity is required for HG-induced GPX1 reduction

Since the kinase activity of TAF1 is responsible for p53 Thr55 phosphorylation,[14] we investigated the role of TAF1 kinase activity in HG-induced p53 phosphorylation and GPX1 reduction in ECs. As indicated in Figure 2*D*, treating cells with the TAF1 kinase inhibitor apigenin effectively blocked HG-induced GPX1 down-regulation at both protein and mRNA levels. To further explore the role of TAF1 in GPX1 down-regulation, we knocked down TAF1 using specific small interfering RNA (TAF1-siRNA) and showed that HG-induced GPX1 down-regulation was abolished under TAF1 abrogation condition (Fig. 2*E*). Importantly, reintroducing siRNA-resistant recoded TAF1 (rcTAF1) but not a TAF1 kinase dead mutant (A2)[18] restored the effects of HG on p53 Thr55 phosphorylation as well as p53 and GPX-1 reduction (Fig. 2*E*). Together, these results suggest that TAF1 kinase activity is critical for HG-mediated GPX1 suppression and endothelial oxidative stress.

To test whether TAF1 kinase activity is directly affected by HG exposure and subsequent ATP increase, we immunoprecipitated TAF1 from HAECs treated with HG in the presence or absence of 2-DG or apigenin, and assayed its kinase activity by measuring p53 Thr55 phosphorylation in vitro. Our results show that TAF1 purified from HG-treated cells undergoes increased p53 Thr55 phosphorylation (Fig. 2*F*), while no increase was observed in the presence of 2-DG or apigenin. To ensure these effects, p53 phosphorylation as well as TAF1 autophosphorylation was confirmed by autoradiogram (Fig. 2*F*). These results suggest the kinase activity of TAF1 is required for HG-induced p53 Thr55 phosphorylation and inactivation, which leads to GPX1 reduction.

Thr55 phosphorylation inhibits GPX1 expression by preventing p53 from binding to the GPX1 promoter

To better elucidate the role of Thr55 phosphorylation in HG-induced GPX1 reduction, we transfected wild type (WT) or T55A mutant p53 into HAECs and subjected the cells to HG treatment. The assay showed HG-induced GPX1 reduction at both mRNA and protein levels were rescued by T55A but not WT (Fig. 3*A*). These observations support the notion that Thr55 phosphorylation is required for HG-induced GPX1 reduction. As p53 is a DNA-bound transcription activator we investigated whether p53 Thr55 phosphorylation affects its ability to bind to the GPX1 promoter in response to HG. As shown in Figure 3*B*, binding of p53 to a p53-binding site (−182 to −163 bp)[26–28] on the GPX1 promoter was indeed observed. Importantly, this binding was reduced upon HG challenge, while inhibition of glucose metabolism by 2-DG or inhibition of TAF1 by apigenin or TAF1-sRNA effectively abolished the reduction. Furthermore, upon HG challenge, reduced occupancy of p53 on the GPX1 promoter was rescued by p53 Thr55 phosphorylation mutant T55A but not wild type p53, suggesting that Thr55 phosphorylation prevents p53 from binding to the GPX1 promoter in response to HG challenge (Fig. 3*C*). Together, these results suggest TAF1-mediated p53 Thr55 phosphorylation is critical for HG-induced GPX1 reduction in HAECs. To ensure that p53-mediated GPX reduction is critical for ROS accumulation in the cell, we established an ectopic GPX1 expression system where GPX1 is expressed under a CMV

promoter and not regulated by p53. As shown in Figure 3*D*, "p53-resistant" GPX1 indeed became resistant to HG challenge and, as a result, antagonized the HG-mediated ROS accumulation. These results imply the TAF1-mediated p53 Thr55 phosphorylation is critical for ROS accumulation under HG conditions. As such, TAF1 may serve as a therapeutic target for diabetic cardiovascular complications to protect endothelial antioxidant defense systems.

TAF1 mediates HG-induced endothelial oxidative stress and apoptosis

Endothelial apoptosis is the final common pathway through which various insults could contribute to the development of certain cardiovascular diseases.[29] Thus, to study the physiological relevance of HG-induced ROS accumulation to endothelial function, we first analyzed endothelial apoptosis by detecting cleaved caspases that play a pivotal role in the execution phase of ROS-triggered apoptosis.[30] HG exposure significantly induces ROS accumulation and caspase-3 activation (cleavage) in HAECs (Fig. 4*A*). Treating cells with 2-DG that blocks glucose metabolism and with PEG-catalase that convert H_2O_2 into water partially blocked cell apoptosis, suggesting glucose metabolism and resultant ROS accumulation play a role in cell apoptosis. Importantly, inhibition of TAF1 by apigenin (Fig. 4*A*) or by TAF1-siRNA (Fig. 4*B*) also partially blocked ROS accumulation and cell apoptosis, suggesting TAF1 is required for HG-induced endothelial cell apoptosis.

To confirm this result, we next assayed the role of TAF1 in HG-induced cells apoptosis by FACS analysis. HG treatment alone causes 14% of cells to undergo apoptosis, while treating cell with HG in the presence of 2-DG or PEG-catalase reduced HG-induced apoptosis to 3.03% or 4.29% respectively (Fig. 4*C*). Further, the combination of HG with the TAF1 inhibitor apigenin also led to a significant decrease in HG-induced apoptosis, suggesting TAF1 plays an important role in the process. Finally, introducing constitutively expressed GPX1 that is independent of p53 regulation (p53-resistant GPX1) into cells also partially blocked HG-induced apoptosis (Fig. 4*C* and Fig. S3). Together, those data clearly support the role of TAF1-mediated p53 phosphorylation in GPX1 reduction and HG-induced endothelial apoptosis.

HG induced TAF1 activation decreases nitric oxide bioavailability and tube formation

Reduced Nitric Oxide (NO) bioavailability and increased oxygen free radical formation can individually or in combination contribute to endothelial dysfunction.[31] A reduction in NO activity occurs very early in experimental and human hyperglycemia, even before any structural changes in the vascular wall.[32, 33] Thus, to further elucidate the pathological relevance of ATP/TAF/p53/GPX1 pathway upon HG challenge, we detected intracellular generation of NO as an index of endothelial function. As reported previously,[34] HG exposure significantly decreased NO production in HAECs (Fig. 5*A*). Importantly, the inhibitory effect of HG was partially reversed by addition of 2-DG, apigenin, catalase, or p53-resistant GPX1, supporting the notion that TAF1 and p53 mediated GPX1 reduction was clearly associated with endothelial dysfunction. Importantly, there was no detectable change in the expression or activation of eNOS (data not shown), suggesting a crucial role for antioxidant enzyme GPX1 in modulating NO bioavailability in HAECs.

NO can trigger increased endothelial cell migration and thereby positively contribute to angiogenesis.[35] We next determined whether GPX1-overexpressing cells were able to retain functional endothelial cell attributes, such as angiogenic responses, during HG exposure. Tube formation assays on Matrigel basement membrane matrix revealed that HAECs incubated with HG formed less extensive tube networks compared to control cells and overexpression of p53-resistant GPX1 significantly recovered this effect. Moreover, the reduced tube formation was also partially rescued by 2-DG, apigenin, catalase or p53-resistant GPX1 (Fig. 5*B*), suggesting the importance of TAF1/p53/GPX1/ROS pathway in high glucose-induced endothelial oxidative stress and dysfunction.

Discussion

In the present study, we presented evidence that HG, via increasing cellular ATP level, activated TAF1 kinase and led to p53 Thr55 phosphorylation. The phosphorylation, in turn, inactivates p53, down-regulates GPX1, and suppresses antioxidant system in vascular endothelium. We also demonstrated that GPX1 down-regulation contributes to HG-induced endothelial oxidative stress, leading to increased endothelial apoptosis as well as impaired NO bioavailability and angiogenic response. Our study unveiled a novel mechanism by which hyperglycemia under the diabetic status causes vascular endothelial dysfunction and potentially provided a therapeutic possibility for diabetes–associated cardiovascular diseases.

In addition to the foregoing mechanism, prolonged HG exposure (6 days) has been shown to reduce SIRT1 protein expression and increase p53 acetylation, which leads to p21 activation and endothelial senescence.[36, 37] It is thus possible that, upon HG exposure, cells undergo a transit p53 inactivation due to increased Thr55 phosphorylation (6–16 hours) and subsequent GPX1 down-regulation, which contributes to generation of ROS and oxidative stress in the cell. If the stress prolongs, endothelial cells will likely call upon additional cell defense system, including SIRT1, which results in sustained hyperacetylation of p53, and potentially SIRT1/p53/p21-mediated endothelial senescence. To test this possibility, we examined SIRT1 expression and p53 acetylation under the condition while reduction of GPX1 level is first observed (16 hours after HG treatment) and found both of them are not affected by HG treatment (Fig. S4). These data suggest that transit p53 inactivation by TAF1 phosphorylation maybe a critical early step in initiation of oxidative stress to the cell and in development of vascular endothelial dysfunction. These data are also in agreement with the finding from a recent functional genome-wide RNAi screening which identified TAF1 as an inducer of apoptosis in response to oxidative stress.[38]

Indeed, hyperglycaemia-induced oxidative stress has been shown a major contributing factor to the development of endothelial dysfunction. Furthermore, increased production of ROS is implicated in the pathogenesis of cardiovascular diseases and diabetic vascular complications.[39, 40] To date, the specific, individual ROS that is most relevant to vascular signaling pathophysiologically is yet identified. Nevertheless, substantial evidence[41, 42] suggests that H_2O_2 is more atherogenic than $O_2^{\bullet -}$ perhaps due to its longer biological life span and ability to diffuse across lipid bilayers.[43] While some $O_2^{\bullet -}$ spontaneously degrades by reacting with NO, $O_2^{\bullet -}$ signal preserved by dismutation into H_2O_2 exerts prolonged

signaling effects. This may explain why direct scavenging H_2O_2 but not $O_2^{\bullet -}$ is more effective in athero-protection. To protect themselves from oxidative damage, cells have developed a sophisticated antioxidant enzyme defense system. In this system, superoxide dismutases (SODs) convert $O_2^{\bullet -}$ into H_2O_2, whereas GPXs and catalase convert H_2O_2 into water.[44] In endothelial cells, H_2O_2 detoxification is primarily mediated by GPX1 as catalase is reportedly not expressed or expressed at very low levels in these cells.[45] GPX1 represents the key antioxidant enzyme in vascular endothelial cells and has been shown to exert a protective effect against the presence of coronary artery disease.[46] GPX1–deficient mice have endothelial dysfunction and abnormal cardiac function after ischemia/reperfusion injury.[47, 48] In clinical studies, GPX1 activity measurements have been found to be predictors of cardiovascular risk in coronary artery disease patients.[49] In the present study, our results reveal that HG dramatically suppresses GPX1 expression by inhibiting its transcription factor p53, leading to intracellular H_2O_2 accumulation. Moreover, we show that GPX1 plays an essential role in preserving endothelial function and NO bioavailability in an eNOS-independent manner (Fig. 5). This result agrees with those by Ulker et al[50] showing that endothelial dysfunction was associated with decreased expression of GPX1 in spontaneous hypertensive rats without change in the expression or activation of eNOS. This may be attributed to the antioxidant actions of GPX1 in removing intracellular H_2O_2, which can induce eNOS uncoupling[51] and augment superoxide production by stimulating NADPH oxidase activation.[52] Taken together, these data strongly support the notion that impairment of antioxidant system GPX1 plays an important role in HG-induced endothelial dysfunction and TAF1-mediated p53 phosphorylation plays a critical role in this process. The fact that the impairment can be reversed by the TAF1 inhibitor apigenin provides an avenue for possible therapy for endothelial dysfunction in type 1 and type 2 diabetes mellitus.

Conclusions

Our study revealed a novel mechanism by which HG induces endothelial oxidative stress and damage through TAF1-mediated, cellular ATP level-regulated p53 Thr55 phosphorylation and subsequent GPX1 inactivation. Furthermore, our results possibly provided an avenue for targeted therapy for diabetes-associated cardiovascular diseases.

Supplementary Material

Refer to Web version on PubMed Central for supplementary material.

Acknowledgments

Funding

This work was supported by the National Cancer Institute at the National Institutes of Health grant CA075180 to X.L.; by American Heart Association postdoctoral fellowship 10POST3530033 and National Institutes of Health SC1CA200517 to Y.W.; and by National Institutes of Health predoctoral fellowship F31CA177219 to S.B.

We are very grateful to B.I. Fragoso, B.J. Gadd and H.C. Zhou for plasmid construction, Drs. W. Sun and Z. Chen for valuable suggestions and helpful discussion.

References

1. The Diabetes Control and Complications Trial Research Group. The effect of intensive treatment of diabetes on the development and progression of long-term complications in insulin-dependent diabetes mellitus. N Engl J Med. 1993; 329:977–986. [PubMed: 8366922]
2. Allen DA, Yaqoob MM, Harwood SM. Mechanisms of high glucose-induced apoptosis and its relationship to diabetic complications. J Nutr Biochem. 2005; 16:705–713. [PubMed: 16169208]
3. UK Prospective Diabetes Study (UKPDS) Group. Intensive blood-glucose control with sulphonylureas or insulin compared with conventional treatment and risk of complications in patients with type 2 diabetes (UKPDS 33). Lancet. 1998; 352:837–853. [PubMed: 9742976]
4. Tesfamariam B, Cohen RA. Free radicals mediate endothelial cell dysfunction caused by elevated glucose. Am J Physiol. 1992; 263:H321–326. [PubMed: 1510128]
5. Langenstroer P, Pieper GM. Regulation of spontaneous EDRF release in diabetic rat aorta by oxygen free radicals. Am J Physiol. 1992; 263:H257–265. [PubMed: 1636763]
6. Vogelstein B, Lane D, Levine AJ. Surfing the p53 network. Nature. 2000; 408:307–310. [PubMed: 11099028]
7. Sharpless NE, DePinho RA. p53: good cop/bad cop. Cell. 2002; 110:9–12. [PubMed: 12150992]
8. Ortega-Camarillo C, Guzman-Grenfell AM, Garcia-Macedo R, Rosales-Torres AM, Avalos-Rodriguez A, Duran-Reyes G, Medina-Navarro R, Cruz M, Diaz-Flores M, Kumate J. Hyperglycemia induces apoptosis and p53 mobilization to mitochondria in RINm5F cells. Mol Cell Biochem. 2006; 281:163–171. [PubMed: 16328969]
9. Fiordaliso F, Leri A, Cesselli D, Limana F, Safai B, Nadal-Ginard B, Anversa P, Kajstura J. Hyperglycemia activates p53 and p53-regulated genes leading to myocyte cell death. Diabetes. 2001; 50:2363–2375. [PubMed: 11574421]
10. Rosso A, Balsamo A, Gambino R, Dentelli P, Falcioni R, Cassader M, Pegoraro L, Pagano G, Brizzi MF. p53 Mediates the accelerated onset of senescence of endothelial progenitor cells in diabetes. J Biol Chem. 2006; 281:4339–4347. [PubMed: 16339764]
11. Merched AJ, Williams E, Chan L. Macrophage-specific p53 expression plays a crucial role in atherosclerosis development and plaque remodeling. Arterioscler Thromb Vasc Biol. 2003; 23:1608–1614. [PubMed: 12842843]
12. Liu B, Chen Y, St Clair DK. ROS and p53: a versatile partnership. Free Radic Biol Med. 2008; 44:1529–1535. [PubMed: 18275858]
13. Sablina AA, Budanov AV, Ilyinskaya GV, Agapova LS, Kravchenko JE, Chumakov PM. The antioxidant function of the p53 tumor suppressor. Nat Med. 2005; 11:1306–1313. [PubMed: 16286925]
14. Li HH, Li AG, Sheppard HM, Liu X. Phosphorylation on Thr-55 by TAF1 mediates degradation of p53: a role for TAF1 in cell G1 progression. Mol Cell. 2004; 13:867–878. [PubMed: 15053879]
15. Gatti A, Li HH, Traugh JA, Liu X. Phosphorylation of human p53 on Thr-55. Biochemistry. 2000; 39:9837–9842. [PubMed: 10933801]
16. Tora L. A unified nomenclature for TATA box binding protein (TBP)-associated factors (TAFs) involved in RNA polymerase II transcription. Genes & development. 2002; 16:673–675. [PubMed: 11963920]
17. Thomas MC, Chiang CM. The general transcription machinery and general cofactors. Critical reviews in biochemistry and molecular biology. 2006; 41:105–178. [PubMed: 16858867]
18. Wu Y, Lin JC, Piluso LG, Dhahbi JM, Bobadilla S, Spindler SR, Liu X. Phosphorylation of p53 by TAF1 inactivates p53-dependent transcription in the DNA damage response. Molecular cell. 2014; 53:63–74. [PubMed: 24289924]
19. Wang L, Sapuri-Butti AR, Aung HH, Parikh AN, Rutledge JC. Triglyceride-rich lipoprotein lipolysis increases aggregation of endothelial cell membrane microdomains and produces reactive oxygen species. Am J Physiol Heart Circ Physiol. 2008; 295:H237–244. [PubMed: 18487440]
20. Li AG, Piluso LG, Cai X, Gadd BJ, Ladurner AG, Liu X. An acetylation switch in p53 mediates holo-TFIID recruitment. Mol Cell. 2007; 28:408–421. [PubMed: 17996705]

21. Berry MJ, Banu L, Chen YY, Mandel SJ, Kieffer JD, Harney JW, Larsen PR. Recognition of UGA as a selenocysteine codon in type I deiodinase requires sequences in the 3′ untranslated region. Nature. 1991; 353:273–276. [PubMed: 1832744]
22. Formoso G, Chen H, Kim JA, Montagnani M, Consoli A, Quon MJ. Dehydroepiandrosterone mimics acute actions of insulin to stimulate production of both nitric oxide and endothelin 1 via distinct phosphatidylinositol 3-kinase- and mitogen-activated protein kinase-dependent pathways in vascular endothelium. Mol Endocrinol. 2006; 20:1153–1163. [PubMed: 16373398]
23. Borradaile NM, Pickering JG. Polyploidy impairs human aortic endothelial cell function and is prevented by nicotinamide phosphoribosyltransferase. Am J Physiol Cell Physiol. 298:C66–74. [PubMed: 19846757]
24. Huang SM, Li J, Harari PM. Molecular inhibition of angiogenesis and metastatic potential in human squamous cell carcinomas after epidermal growth factor receptor blockade. Mol Cancer Ther. 2002; 1:507–514. [PubMed: 12479268]
25. Brown J. Effects of 2-deoxyglucose on carbohydrate metablism: review of the literature and studies in the rat. Metabolism. 1962; 11:1098–1112. [PubMed: 13873661]
26. Krieg AJ, Hammond EM, Giaccia AJ. Functional analysis of p53 binding under differential stresses. Mol Cell Biol. 2006; 26:7030–7045. [PubMed: 16980608]
27. Tan M, Li S, Swaroop M, Guan K, Oberley LW, Sun Y. Transcriptional activation of the human glutathione peroxidase promoter by p53. J Biol Chem. 1999; 274:12061–12066. [PubMed: 10207030]
28. Jen KY, Cheung VG. Identification of novel p53 target genes in ionizing radiation response. Cancer Res. 2005; 65:7666–7673. [PubMed: 16140933]
29. Stefanec T. Endothelial apoptosis: could it have a role in the pathogenesis and treatment of disease? Chest. 2000; 117:841–854. [PubMed: 10713015]
30. Matsura T, Kai M, Fujii Y, Ito H, Yamada K. Hydrogen peroxide-induced apoptosis in HL-60 cells requires caspase-3 activation. Free radical research. 1999; 30:73–83. [PubMed: 10193575]
31. Ignarro LJ, Cirino G, Casini A, Napoli C. Nitric oxide as a signaling molecule in the vascular system: an overview. J Cardiovasc Pharmacol. 1999; 34:879–886. [PubMed: 10598133]
32. Vallance P, Chan N. Endothelial function and nitric oxide: clinical relevance. Heart. 2001; 85:342–350. [PubMed: 11179281]
33. Bohlen HG, Nase GP. Arteriolar nitric oxide concentration is decreased during hyperglycemia-induced betaII PKC activation. Am J Physiol Heart Circ Physiol. 2001; 280:H621–627. [PubMed: 11158959]
34. Cai S, Khoo J, Channon KM. Augmented BH4 by gene transfer restores nitric oxide synthase function in hyperglycemic human endothelial cells. Cardiovasc Res. 2005; 65:823–831. [PubMed: 15721862]
35. Chin K, Kurashima Y, Ogura T, Tajiri H, Yoshida S, Esumi H. Induction of vascular endothelial growth factor by nitric oxide in human glioblastoma and hepatocellular carcinoma cells. Oncogene. 1997; 15:437–442. [PubMed: 9242380]
36. Arunachalam G, Samuel SM, Marei I, Ding H, Triggle CR. Metformin modulates hyperglycaemia-induced endothelial senescence and apoptosis through SIRT1. Br J Pharmacol. 2014; 171:523–535. [PubMed: 24372553]
37. Zhang E, Guo Q, Gao H, Xu R, Teng S, Wu Y. Metformin and resveratrol inhibited high glucose-induced metabolic memory of endothelial senescence through SIRT1/p300/p53/p21 pathway. PLOS ONE. 2015; 10:e0143814. [PubMed: 26629991]
38. Kimura J, Nguyen ST, Liu H, Taira N, Miki Y, Yoshida K. A functional genome-wide RNAi screen identifies TAF1 as a regulator for apoptosis in response to genotoxic stress. Nucleic Acids Res. 2008; 36:5250–5259. [PubMed: 18684994]
39. Cai H. NAD(P)H oxidase-dependent self-propagation of hydrogen peroxide and vascular disease. Circ Res. 2005; 96:818–822. [PubMed: 15860762]
40. Brandes RP, Kreuzer J. Vascular NADPH oxidases: molecular mechanisms of activation. Cardiovasc Res. 2005; 65:16–27. [PubMed: 15621030]

41. Khatri JJ, Johnson C, Magid R, Lessner SM, Laude KM, Dikalov SI, Harrison DG, Sung HJ, Rong Y, Galis ZS. Vascular oxidant stress enhances progression and angiogenesis of experimental atheroma. Circulation. 2004; 109:520–525. [PubMed: 14744973]
42. Cai H. Hydrogen peroxide regulation of endothelial function: origins, mechanisms, and consequences. Cardiovasc Res. 2005; 68:26–36. [PubMed: 16009356]
43. Paravicini TM, Touyz RM. Redox signaling in hypertension. Cardiovasc Res. 2006; 71:247–258. [PubMed: 16765337]
44. Li S, Yan T, Yang JQ, Oberley TD, Oberley LW. The role of cellular glutathione peroxidase redox regulation in the suppression of tumor cell growth by manganese superoxide dismutase. Cancer Res. 2000; 60:3927–3939. [PubMed: 10919671]
45. Zhang Y, Handy DE, Loscalzo J. Adenosine-dependent induction of glutathione peroxidase 1 in human primary endothelial cells and protection against oxidative stress. Circ Res. 2005; 96:831–837. [PubMed: 15802613]
46. Flohe L. Glutathione peroxidase. Basic Life Sci. 1988; 49:663–668. [PubMed: 3074794]
47. Forgione MA, Cap A, Liao R, Moldovan NI, Eberhardt RT, Lim CC, Jones J, Goldschmidt-Clermont PJ, Loscalzo J. Heterozygous cellular glutathione peroxidase deficiency in the mouse: abnormalities in vascular and cardiac function and structure. Circulation. 2002; 106:1154–1158. [PubMed: 12196344]
48. Forgione MA, Weiss N, Heydrick S, Cap A, Klings ES, Bierl C, Eberhardt RT, Farber HW, Loscalzo J. Cellular glutathione peroxidase deficiency and endothelial dysfunction. Am J Physiol Heart Circ Physiol. 2002; 282:H1255–1261. [PubMed: 11893559]
49. Schnabel R, Lackner KJ, Rupprecht HJ, Espinola-Klein C, Torzewski M, Lubos E, Bickel C, Cambien F, Tiret L, Munzel T, Blankenberg S. Glutathione peroxidase-1 and homocysteine for cardiovascular risk prediction: results from the AtheroGene study. J Am Coll Cardiol. 2005; 45:1631–1637. [PubMed: 15893179]
50. Ulker S, McMaster D, McKeown PP, Bayraktutan U. Impaired activities of antioxidant enzymes elicit endothelial dysfunction in spontaneous hypertensive rats despite enhanced vascular nitric oxide generation. Cardiovasc Res. 2003; 59:488–500. [PubMed: 12909332]
51. Chalupsky K, Cai H. Endothelial dihydrofolate reductase: critical for nitric oxide bioavailability and role in angiotensin II uncoupling of endothelial nitric oxide synthase. Proceedings of the National Academy of Sciences of the United States of America. 2005; 102:9056–9061. [PubMed: 15941833]
52. Li WG, Miller FJ Jr, Zhang HJ, Spitz DR, Oberley LW, Weintraub NL. H(2)O(2)-induced O(2) production by a non-phagocytic NAD(P)H oxidase causes oxidant injury. J Biol Chem. 2001; 276:29251–29256. [PubMed: 11358965]

Highlights

- Treating endothelial cells with high glucose increased cellular ATP level, resulting in activation of TAF1 kinase and p53 Thr55 phosphorylation
- Thr55 phosphorylated p53 dissociates from the GPX1 promoter, leading to reduction of GPX1 expression and suppression of antioxidant system
- The p53 phosphorylation mediated GPX1 reduction plays a role in endothelial dysfunction under high glucose condition

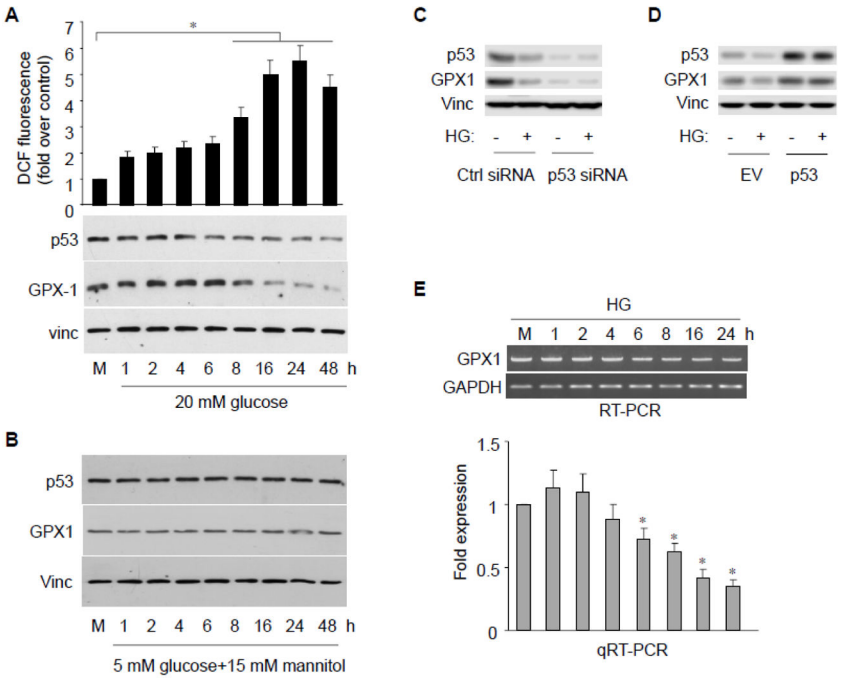

Fig. 1.

High glucose exposure inhibits GPX1 and increases ROS formation in endothelial cells. A, B, HAECs were treated with high glucose (20 mM) or with osmotic control (5 mM glucose + 15 mM mannitol) at various times. The p53 and GPX1 protein were assayed by immunobloting. Intracellular ROS was assessed by fluorescence intensity of dichlorofluorescin (DCF fluorescence) emission. Data are presented as mean fold increases (±SD) in treated groups over basal values from three independent experiments. *p<0.05 versus controls. C, HAECs were transfected with either p53 or control siRNA. The p53 and GPX1 protein were assayed by immunobloting. D, HAECs were transfected with either p53 or empty vector (EV). The p53 and GPX1 protein were assayed by immunobloting. E, RT-PCR or qRT-PCR analysis reveals GPX1 mRNA levels at the time points following HG treatment. The blot is a representative of 3 blots from 3 independent experiments (n = 3 each). Results are expressed as mean ± SD. *p<0.05 vs. control.

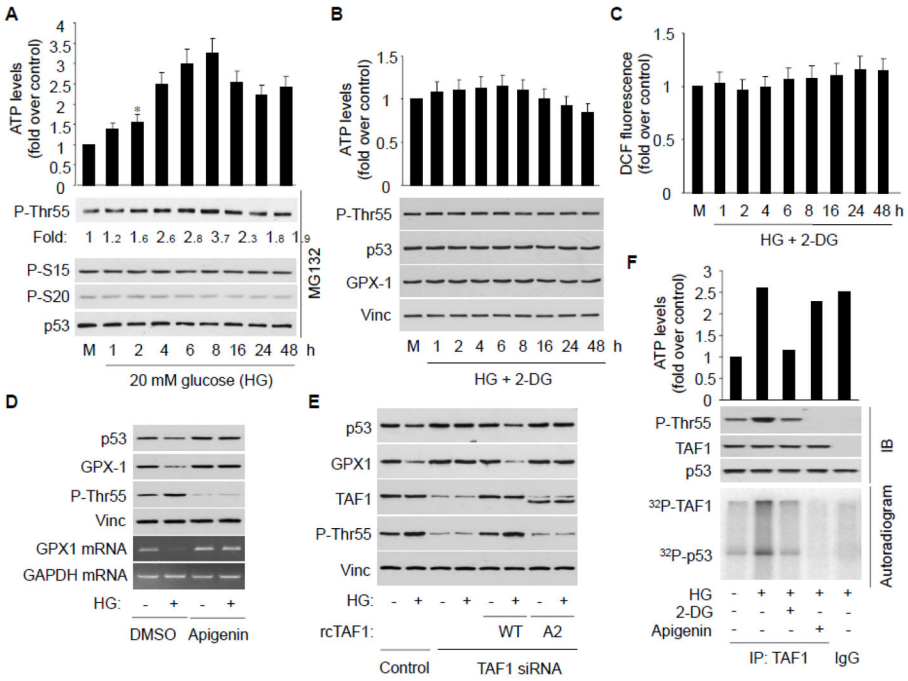

Fig. 2.

Increased cellular ATP level is responsible for TAF1 activation, p53 Thr55 phosphorylation, GPX1 reduction, and ROS formation. A, HAECs were treated with 20 mM glucose, as well as MG132 to normalize the p53 protein level. Ser15, Ser20 and Thr55 phosphorylated p53 were detected using corresponding phospho-specific antibody. The intracellular ATP levels were determined using a luciferin/luciferase method according to manufacturer's protocol. Bars represent mean fold increases (±SD) in treated groups over basal values from 3 independent experiments. The blot is a representative of 3 blots from 3 independent experiments. *p<0.05 vs. control. B, C, HAECs were treated with 20 mM HG in the presence of 2-DG. Following the treatment, cells were harvested for detection of p53 phosphorylation and p53 and GPX1 protein, as well as for determination of intracellular ROS (n = 3 each). D, HAECs were incubated with HG in the presence of DMSO or apigenin. p53, GPX-1 and Thr55 phosphorylated p53 were detected by immuneblotting. p53 GPX1 mRNA was detected by RT-PCR (n = 3 each). E, HUVECs were transfected with TAF1–specific or control siRNA, with or without recoded wild type TAF1 (WT rcTAF1) or kinase dead mutant (A2) as indicated. p53, GPX1, TAF1 protein level as well as Thr55 phosphorylation were detected by immunobloting (n = 3 each). F, HAECs were treated with HG in the presence or absence of 2-DG and apigenin as indicated, TAF1 was immunoprecipitated and in vitro TAF1 kinase assay was carried out using baculovirus expressed and purified p53. TAF1 and p53 phosphorylation were detected by either autoradiograph or immunobloting as indicated (n = 3 each).

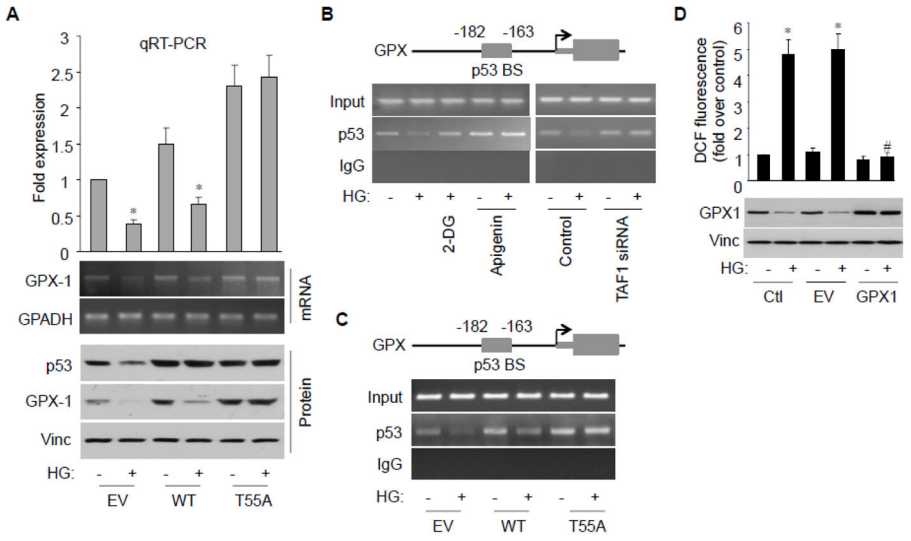

Fig. 3.

Thr55 phosphorylation inhibits p53 binding to the GPX1 promoter. A, HAECs were transfected with either empty vector (EV), wild-type p53 or T55A and treated with HG. GPX1 mRNA levels were analyzed by RT-PCR or qRT-PCR. B, HAECs were incubated with HG in the presence or absence of 2-DG or apigenin, control or TAF1 siRNA transfection, and subject to ChIP assay. p53 binding site indicated on the top was amplified by PCR. PCR products were resolved by agarose gel electrophoresis and visualized by ethidium bromide staining. C, HAECs were transfected with empty vector (EV), wild-type p53, or T55A and treated with HG. ChIP analysis of p53 binding to the GPX promoter was assayed. D, HAECs were transfected with either empty vector (EV) or GPX-1 expression construct and treated with HG. Intracellular ROS was assessed by the fluorescence intensity of DCF emission. Data are presented as mean fold increases (±SD) in treated groups over basal values from 4 independent experiments. *p<0.01 vs. control; #p<0.01 vs. HG group.

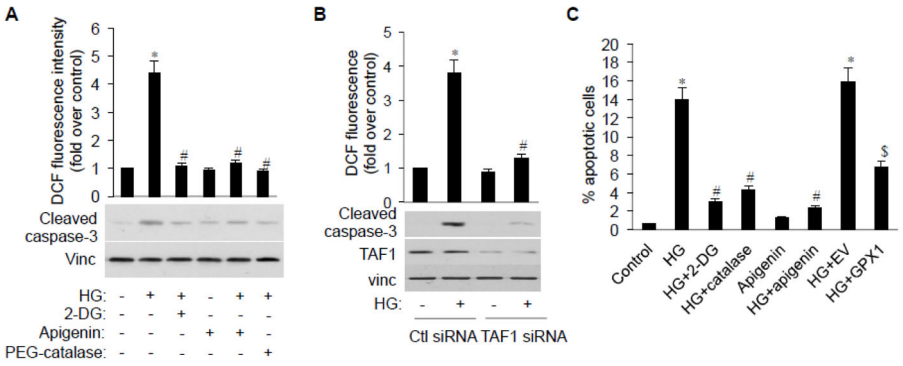

Fig. 4.

TAF1 inhibition ameliorates HG-induced H_2O_2 accumulation and endothelial apoptosis. A, HAECs were incubated with HG in the presence or absence of 2-DG, apigenin or PEG-catalase. Cleaved caspase-3 was assayed by immunobloting. Intracellular ROS was analyzed as mentioned above. *p<0.01 vs. control; #p<0.01 vs. HG/control siRNA. B, HAECs were transfected with control or TAF1 siRNA and treated with HG. Intracellular ROS and cleaved caspase-3 levels were analyzed as mentioned above. *p<0.01 vs. control; #p<0.01 vs. HG/control siRNA. C, HAECs were treated with HG in the presence or absence of 2-DG, apigenin or PEG-catalase, EV or GPX1 transfection and processed for FACS analysis for apoptotic cells (subG1) according to DNA content (PI staining). Bar graphs represent mean ± SD of three independent experiments. * p<0.01 vs. control; # p<0.01 vs. HG; $ p<0.01 vs. HG+EV.

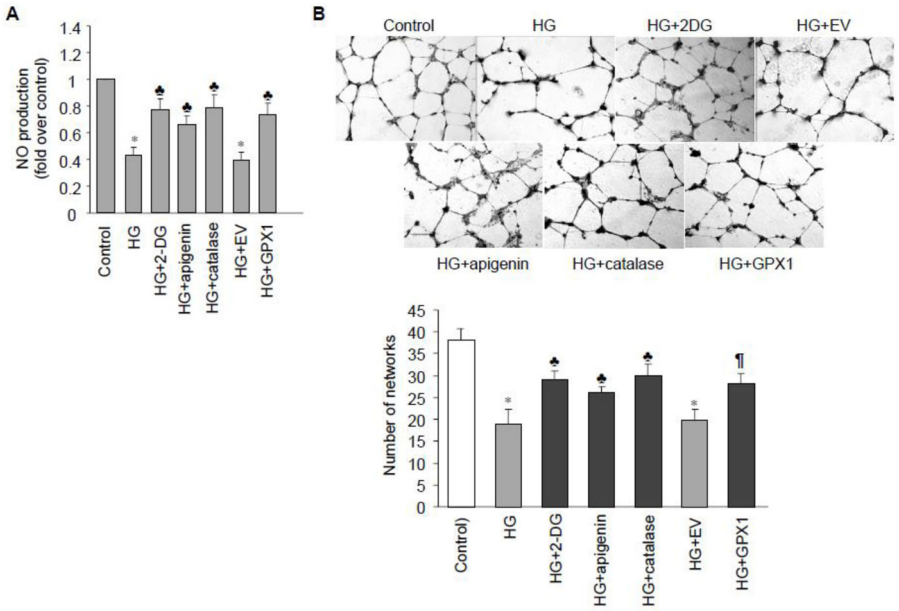

Fig. 5.

TAF1 inhibition alleviates HG-induced decrease in endothelial nitric oxide bioavailability and tube formation. A, HAECs were incubated with HG in the presence or absence of 2-DG, apigenin or PEG-catalase and NO production from 4 independent experiments were assessed using DAF-2/DA as described. Quantitative results corrected by protein concentrations were shown. The results are represented as mean fold increases (±SD) in treated groups over basal values. * p<0.05 vs control; ♣ p<0.05 vs HG or HG+EV. B, Young HAEC populations were seeded on Matrigel basement membrane matrix in growth media with either 5 mM (control) or 20 mM glucose (HG) in the presence or absence of 2-DG, apigenin, catalase or GPX1 overexpression. Tube network formation was monitored by microscopy (×100 magnification) (upper panel) and quantified by counting capillary-like networks per field of view (lower panel). n = 3; * p < 0.05 vs. control; ♣ p < 0.05 vs. HG or HG + EV.